CFD Simulation on Aerodynamic Performance of Hyperloop Vehicle

Repalli Satya Venkat Narayan Murty[1], Pranav Pabsetti[1], Jai Bhoje[1], Harish Rajan[1,*]

[1] School of Mechanical Engineering, Vellore Institute of Technology, Chennai, Tamil Nadu 600127, India

ARTICLE INFO	ABSTRACT
          	Aerodynamic drag is one of the most opposing factors for ground vehicle. This becomes even more difficult while travelling through a tunnel. The Evacuated-Tube Trains (ETTs) or Hyperloop's are a new concept of ground transportation presently being developed by many different companies. The main purpose of an Hyperloop can be displayed as a cheaper medium of ground transport, which could allow its consumers to propagate to different places at a cheaper and faster rate compared to the present day locomotives and road transport. Passengers can travel at over 700 mph in floating capsules that swoop along within gigantic low-pressure tubes that are either below or above surface. This study analyses the Hyperloop designs using Computational Fluid Dynamics software ANSYS FLUENT. The effects of operating speed, Capsule shape and internal tube pressure have been studied in this paper. The flow inside the tube is considered as turbulent and incompressible. The software simulation results show the significant effects of inside pressure and operating speed on the aerodynamic drag of the capsule. Study with different shapes for the Capsule's front and rear end suggest the most optimum shape for least aerodynamic drag.

1. Introduction

Elon Musk, the project's main proponent, claims that Hyperloop seeks to be a new method of transportation, the fifth after aircraft, trains, automobiles, and boats, that should be more economical, more convenient, resistant to earthquakes, resistant to intense climatic conditions and safe for those residing nearby. The traditional high-speed trains is regarded as being slower, expensive to operate, and two orders of magnitude less safe than flying, yet it is seen as an alternative state-wide mass transit system to driving or flying for distances under 1500 km . The 2013's promotion of the concept on Hyperloop and followed by a design competition three years later and student team pod competition which were held in the later years that is 2017, 2018 at SpaceX Hawthrone, on specifically a 1.6-kilometer-long, 1.83-meter diameter partial-vacuum test tube track, have sparked a significant amount of new R&D by the consultants, scientists, students and many start-ups around the world was showed by Hansen [1]. It is anticipated that a number of

---

* *Corresponding author.*
E-mail address: harish.r@vit.ac.in

variables will enable Hyperloop technology to improve convenience and shorten travel times between adjacent cities. A significant component is the high speed made possible by the system architecture, which can cruise at up to 700 miles per hour. This is comparable to or quicker than air travel, and it is significantly faster than automobiles or rail systems. Location and accessibility are further factors. The goal of an Hyperloop system is to cut travel time compared to air travel by removing or drastically lowering time spent at either end of the route. Although Hyperloop systems may have certain benefits, they also have some downsides. In addition to those previously stated, these include the manufacturing of pods and the extensive purchase of supporting equipment; the prices are mostly unknown and might be significant. Opgenoord and Caplan [2] offered an improvement to the Massachusetts Institute of Technology team's Hyperloop pod. The proposed speed was Mach 0.3, another factor which was analyzed is the transonic speed by which they understood the results of the influence of choke flow all around the Hyperloop vehicle on the drag force. Due to the decreasing atmospheric pressure, the air density within the tube reduces at a fixed temperature. This aids in lowering the aerodynamic drag that Hyperloop capsules inside tubes suffer. Zhou *et al.,* [3] made levitation possible in the Hyperloop by utilizing strong electromagnets. In the alternative, air bearings that are continually fed compressed air can also be employed to lift the tube. The Hyperloop capsules are propelled in the transonic speed zone by linear accelerators positioned at carefully chosen strategic places.

1.1 Literature Review

The term "Hyperloop" is one of the theoretical high-speed transportation system, which was first proposed by Elon Musk. The capsules with passengers propel through low-pressure tubes at insane speeds being powered by linear induction motor and air compressors [4,5]. This type of transportation almost feels like cruising in air. Higher cruising speeds are often accompanied with several number of aerodynamic restrictions, such as involvement of compressibility effects, development of shockwaves and subsequent aerodynamic drag and reaching the kantrowitz limit. Musk's team has bought an idea of installing an air compressor on the head of the capsule to pump air that which will flow surrounding the capsule and to the bypass nozzle which is installed at the rear end in order to circumvent these limits faced when the flow of air all around the capsule is blocked. This instead reduces the volume of air which must flow all around the sides of the capsule, allowing the capsules velocities to reach the speeds of Mach 1 [4,5]. Sui *et al.,* [6] investigated the impact of shock waves on maglev trains in an evacuated environment and found that mild shock waves were present at the back of the train in the range of velocities comparable to Mach no. M = 0.57 with blockage ratio = 0.5. Yang *et al.,* [7] explained few concepts about evacuated tube transports. The idea of a transportation system using evacuated tubes has several benefits, including low energy consumption, increased speed, lower noise pollution, lower aerodynamic resistance, etc. [8-10]. Zhang *et al.,* [11] outlined a few important problems with evacuated tube transportation systems that need to be taken into account during the design phase. Lluesma-Rodríguez *et al.,* [12] outlined on what would happen in a closed and controlled environment of a ETT which can be written as Evacuated tube train.

Yang *et al.,* [7] in this paper in order to examine the optimization approach for the parameter design of the vehicle body, this work uses numerical simulations based on the finite volume method. According to the findings, the optimized vehicle's aerodynamic resistance is further decreased, the drag reduction rate reaches 5.52%, and the speed at which the Kantrowitz limit phenomena occurs is postponed from 760 to 860 km/h. Chen *et al.,* [13] did their investigation on maglev trains with varying shapes. However, they were mainly focused on pressure difference

between head and tail of the trains which in essence is the significant reason for aerodynamic pressure drag generation. Ehrendorfer *et al.,* [14] explained the compression and expansion waves that are produced as the train enters the tunnel are one of these issues. In order to create a standard HSR, this circumstance must be taken into account. Although this issue has been studied by other writers as well, the author focused on this entrance effect. Kwon *et al.,* [15] optimized the train's nose shape and reduced the tunnel compression wave using the response surface approach and axisymmetric compressible Euler equations. Significant findings were also made by Liu *et al.,* [16], who stated that the friction drag is considerably less than the pressure drag. Additionally, they observed that the BR significantly affects the aerodynamic and pressure drag coefficients, which do not fluctuate with tube pressure. With pressure and approximately squarely with train speed, the drag itself changed linearly. Jia *et al.,* [17] investigated the Pressure Recycle Ducts (PRD) and how the interval length and opening width of the PRD affected the differential pressure. Bao *et al.,* [18] examined the impact of the tube train's temperature from 243 K to 393 K at 0.1 atm. They claimed that as the Mach number rises at a specific speed, 1000 km/h, supersonic phenomena become more severe when the temperature is reduced. High tube temperatures accelerate sound, which lowers the Mach number for the same pod speed and delays choking while lowering aerodynamic drag. Chu *et al.,* [19] did investigation of the pressure waves produced while two trains passed each other in a tunnel employed a three-dimensional and compressible turbulence model. According to Kim and Rho [20], because of their superposition and propagation, the pressure waves of a high-speed train through a tunnel exhibit complex fluctuations. Research on the wave phenomena caused by a super-fast evacuated tube maglev train was conducted by Zhou *et al.,* [21]. The production and evolution process of aerodynamic heating in the tube was lastly examined by Niu *et al.,* [22]. The danger of choking, which is defined by the minimal section between the capsule and the inner tube wall, was estimated by Kale *et al.,* [23] in 2015 when they presented an overall system of the Hyperloop idea. Pathan *et al.,* [24] have developed a similar mesh for a 2D axisymmetric geometry. Gan *et al.,* [25] used CFD analysis to predict drag coefficients and plot velocity contours. In the literature, several authors have conducted CFD simulations to predict lift and drag coefficients [26-28].

The objective of this paper is to carry out 2-Dimensional CFD simulations of a particular flow field around the Hyperloop capsule and compare between 4 different shapes for the capsule model (Rectangular, Linear, Semicircular and Elliptical). The comparison between the different types of the capsule model used in differentiating the Aerodynamic drag, Velocity distribution and Pressure distribution, which helped us in determining the optimum capsule model. ANSYS Fluent was used to analyze the different capsule models using a 2D axisymmetric model. The results were analyzed to conclude the most optimum shape for the capsule.

2. Numerical Model
2.1 Design Parameters

The parameters for the design in our research for the Hyperloop system are based on the Trans rapid International Maglev train which was proposed by Elon Musk and SpaceX. The design parameters are below

  i. The capsule has a designed speed of 800Km/h in the Hyperloop system.
  ii. One basic assumption taken is that the tube is to be partially evacuated to 2000 Pa at temperature of 293 K.

iii. The dimensions of the capsule in which the length of the capsule is fixed at 30 m and height at 1.5 m, while the length of the rear and front portion depends upon the design style of its respective ends.
iv. Musk *et al.,* [4] stated that the diameter of the inner portion of the tube is set to 2.5 m with a blockage ratio of 0.36 has been selected as per the suggestions in Hyperloop alpha paper.

2.2 Basic Assumptions

The following assumptions are considered for the modeling and numerical simulation of aerodynamic flow over a hyperloop vehicle. The selection of turbulence model, Mach number and operating temperature are listed below.

i. Subjected to the design speeds of the Hyperloop capsule, the flow is considered turbulent as the Reynold's number in the flow field is greater than 10^5. To simulate the flow field, a k-epsilon Realizable turbulence model is employed [29-31].
ii. Pandey and Mukherjea [32] stated that for Mach number (M) < 0.3 the assumption was taken that the flow inside the tube is incompressible. For M>0.3 the flow inside the tube was compressible.
iii. An assumption is taken that the tube temperature is 293 K, and to remain constant.
iv. This study deals with a two-dimensional simulation. The calculation plane is chosen to be the longest longitudinal portion of the capsule, and the capsule is considered to be flawlessly smooth with no seams, gaps, or other surface flaws.
v. Since the Hyperloop pods are magnetically levitated, friction is at a minimum. Thus, aerodynamic drag is the sole challenge the Hyperloop pod faces.

2.3 Mathematical Model

For the modelling of the fluid flow of the Hyperloop system, the conventional K-epsilon two equation turbulence model of incompressible, stable, and viscous fluid flow in 2-D was used. The following is a presentation of the governing equations for the mathematical modelling of fluid flow

Continuity equation

$$\nabla.U = 0 \tag{1}$$

U = Velocity vector of the flow field in m/s

Conservation of momentum equation

$$\nabla.(\rho u U) = \nabla.(\rho \nabla u) - \frac{\partial p}{\partial x} \tag{2}$$

ρ = Density of air in Kg/m³
p = Pressure of flow field in Pa
u = x component of U
U = Velocity vector of the flow field in m/s

Kinetic energy turbulence equation

$$\nabla.(\rho k U) = \frac{\partial}{\partial y}[(\mu_1 + \frac{\mu_t}{\sigma_k})\frac{\partial k}{\partial y}] + \mu_t(\frac{\partial u}{\partial y} + \frac{\partial v}{\partial x})\frac{\partial v}{\partial x} - \rho\varepsilon \tag{3}$$

where,

P = Density of air in Kg/m^3
U = Velocity vector of the flow field in m/s
U = x-component of U
v = y-component of U
k = Turbulence kinetic energy in J/Kg
μ1 = Coefficient of viscosity for laminar flow in N.s/m^2
$\mu t = \rho C_\mu k^2/\varepsilon$
σ_k = 1.0
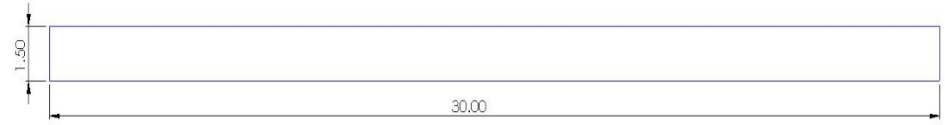E = Rate of Turbulence Dissipation in J/Kg
u = x component of U

Kinetic Energy dissipation rate turbulence equation

$$\nabla.(\rho\varepsilon U) = \nabla.(\rho\nabla u) - \frac{\partial}{\partial y}[(\mu_1 + \frac{\mu_t}{\sigma_\varepsilon})\frac{\partial\varepsilon}{\partial y}] + \frac{\varepsilon}{k}C_1\mu_t\frac{\partial v}{\partial x}(\frac{\partial u}{\partial y} + \frac{\partial v}{\partial x}) - C_2\rho\frac{\rho^2}{k} \tag{4}$$

ρ = Density of air in Kg/m^3
U = Velocity vector of the flow field in m/s
u = x-component of U
v = y-component of U
k = Turbulence kinetic energy in J/Kg
μ1 = Coefficient of viscosity for laminar flow in N.s/m^2
C1 = 1.47
C2 = 1.92
$\mu t = \rho C_\mu k^2/\varepsilon$
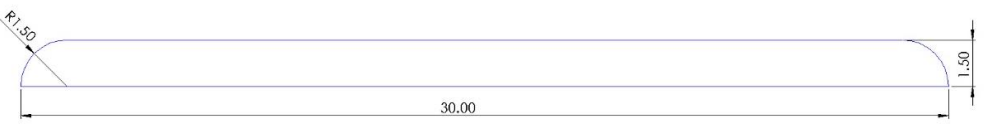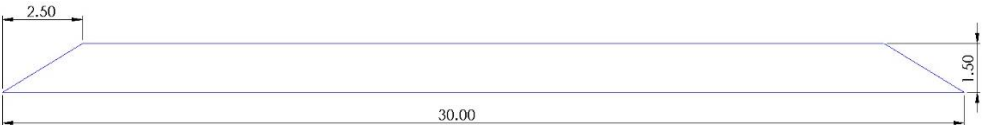σ_k = 1.0
σ_ε = 1.3
ε = Rate of Turbulence Dissipation in J/Kg
u = x component of U

2.4 Capsule Models

In this research, four different types of shapes were used to perform the analysis. The 4 different shapes are classified as Semicircle, Rectangle, Ellipse and Linear (2:1). Table 1 indicates the different geometrical configurations (Rectangular, Linear, Semi-circular and Elliptical) of the Hyperloop capsule considered in the numerical simulations.

Table 1
Different models of capsules

Shape	Capsule models
Rectangle	
Semicircle	
Linear	
Ellipse	

2.5 Computational Domain

The computational domain model is shown in Figure 1, the tube diameter is 2.5m and the entire tube length is 60m. The total length of the capsule is 30m and the pod diameter is (1.5m) in accordance with the blockage ratio value of 0.36. The distance from the front boundary to inlet of the capsule and rear boundary to the outlet of capsule is 15m.
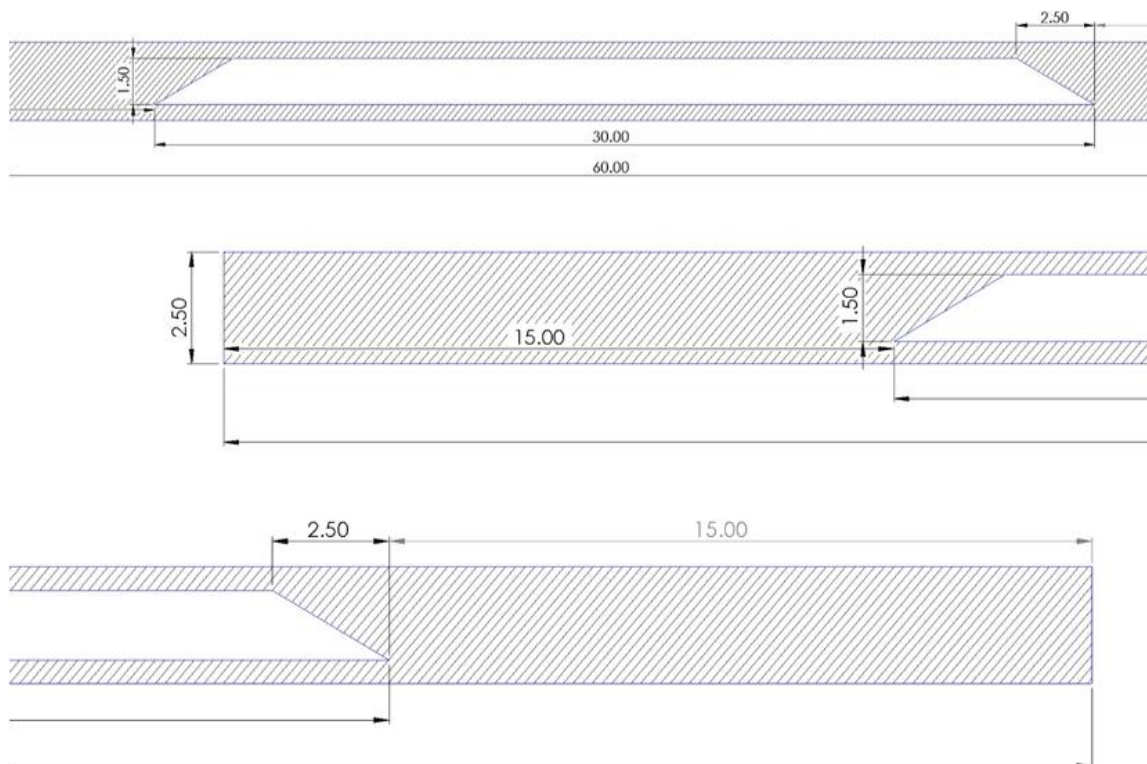
Fig. 1. Schematic of the Computational model

2.6 Computational Meshing

Figure 2 represents the mesh generated for a Hyperloop model. Versteeg and Malalasekera [33] found that in computational fluid dynamics, the geometry of the problem is discretized in order to find the solution of partial differential equations. The governing equations are essentially approximated over the nodes and elements that make up the problem geometry.
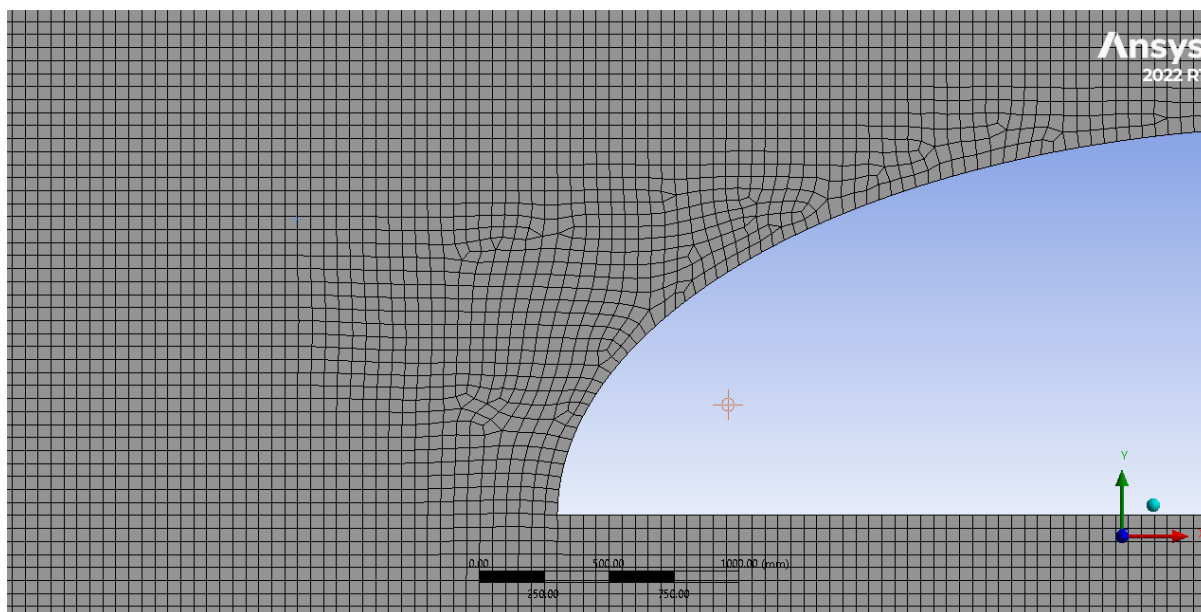

Fig. 2. Mesh generated for the Hyperloop capsule with Nodes = 44549; Elements = 42693

2.7 Boundary Conditions

The left wall of the capsule body is specified as the Inlet boundary condition with flow velocity of 800 km/h and the right end of the capsule is specified with an Outflow boundary condition. The tube is in static and adiabatic boundary condition. "No slip conditions" is selected for the Hyperloop wall border. The pressure inside the tube is 2000Pa, and the Blockage ratio considered is 0.36.

2.8 Simulation Cases

The capsule models have been simulated based on Eq. (1) to Eq. (4) as governing equations for four types of shapes classified for the capsule. The software used is ANSYS Fluent software. The simulations are developed to provide the analysis on Velocity profile, Pressure profile and Force results.

i. The velocity profile shows the deviation in velocity of fluid around the Hyperloop capsule in a closed tube, and the points with peaked velocity has been determined.
ii. The pressure profile shows the deviation in pressure of fluid around the Hyperloop capsule in a closed tube, and the points with peaked velocity has been determined.
iii. The force data demonstrate how much drag is produced on the capsule surface by fluid flow.

Table 2 indicates the turbulence model, turbulence parameters, operating pressure for the fluid entering through the inlet.

Table 2
ANSYS fluent settings for CFD simulations

Parameters	Value
Turbulence model	k-epsilon realizable
Turbulence parameters	Turbulence intensity= 5%, Turbulence viscosity ratio= 10
Operating pressure(pa)	2000
Flow type	Rhie-chow: Distance based
Gradient reconstruction scheme	Least square cells based
Convection scheme	Second order upwind
Convergence criterion	Maximum residual less than 10^{-6} & iteration number greater than 1000

3. Results and Analysis

3.1 Velocity and Pressure Contours for Rectangular Capsule Model

On the basis of results obtained from simulation of Rectangular shaped capsule model, velocity contour and pressure contour have been presented in Figure 3 and Figure 4 respectively. The maximum fluid flow velocity is observed on the edges of head of the capsule which is 863 m/s. In Figure 4, the pressure is maximum in the upstream side of the vehicle, where the capsule model restricts the smooth flow of pressure around the surface of the capsule. This obstruction caused in the flow of fluid generates a maximum fluid flow pressure of 2.23×10^5 Pa on front of the capsule.
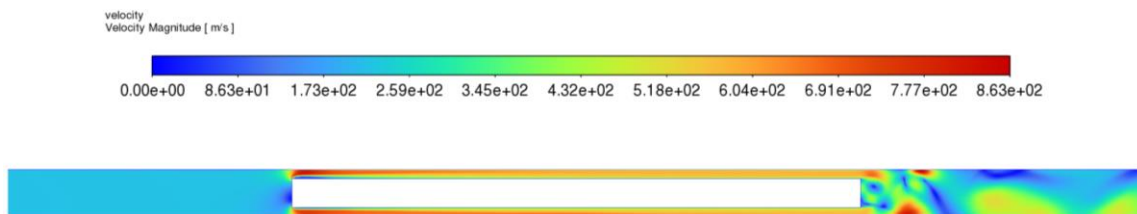

Fig. 3. Rectangular Capsule model: Velocity contour(Max. Velocity = 863 m/s)
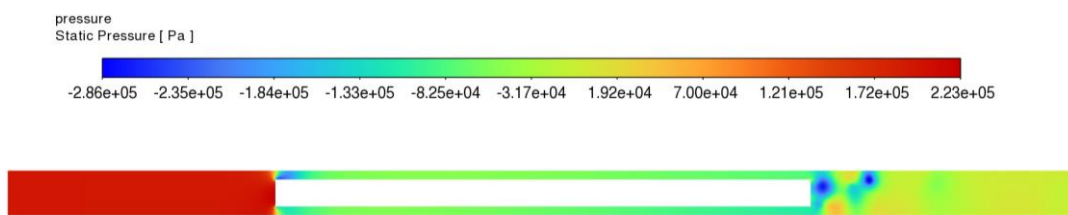

Fig. 4. Rectangular Capsule model: Pressure contour(Max. Pressure = 2.23 x 10^5 Pa)

3.2 Velocity and Pressure Contours for Linear Capsule Model

On the basis of results obtained from simulation of Linear shaped capsule model, velocity contour and pressure contour have been presented in Figure 5 and Figure 6 respectively. In Figure 5, the maximum intensity of flow field velocity is observed on top of the Hyperloop vehicle which is 674 m/s, and in Figure 6 the pressure is dropping on the downstream side of the Hyperloop vehicle. The maximum fluid flow pressure of 1.13 x 10^5 Pa is observed in front of the capsule because of direct impact of air on the Hyperloop capsule's head.

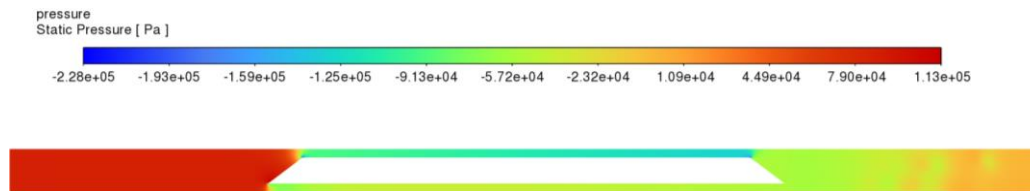**Fig. 5.** Linear Capsule model: Velocity contour(Max. Velocity = 674 m/s)

Fig. 6. Linear Capsule model: Pressure contour(Max. Pressure = 1.13 x 10^5 Pa)

3.3 Velocity and Pressure Contours for Semicircular Capsule Model

On the basis of results obtained from simulation of Linear shaped capsule model, velocity contour and pressure contour have been presented in Figure 7 and Figure 8 respectively. In Figure 7, the maximum intensity of flow field velocity is observed on top of the Hyperloop vehicle which is 634 m/s, and in Figure 8, the pressure is dropping on the downstream side of the Hyperloop vehicle. The maximum fluid flow pressure of 8.60 x 10^4 Pa is observed in front of the capsule because of direct impact of air on the Hyperloop capsule's head.

Fig. 7. Semicircular Capsule model: Velocity contour(Max. Velocity = 634 m/s)

Fig. 8. Semicircular Capsule model: Pressure contour(Max. Pressure = 8.60 x 10^4 Pa)

3.4 Velocity and Pressure Contours for Elliptical Capsule Model

On the basis of results obtained from simulation of Linear shaped capsule model, velocity contour and pressure contour have been presented in Figure 9 and Figure 10 respectively. In Figure 9, the maximum intensity of flow field velocity is observed on top of the Hyperloop vehicle which is 633 m/s, and in Figure 10, the pressure is dropping on the downstream side of the Hyperloop vehicle. The maximum fluid flow pressure of 7.78 x10^4 Pa is observed in front of the capsule because of direct impact of air on the Hyperloop capsule's head.
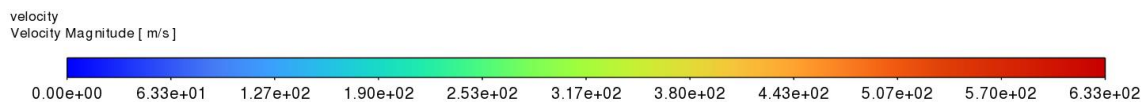
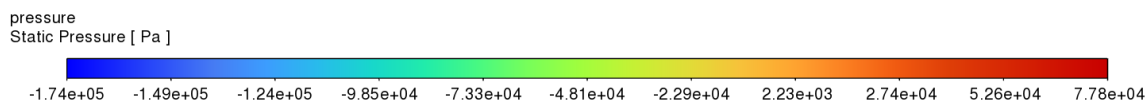**Fig. 9.** Elliptical Capsule model: Velocity contour(Max. Velocity = 633 m/s)

Fig. 10. Elliptical Capsule model: Pressure contour(Max. Pressure = 7.78 x 10^4 Pa)

Figure 11 shows the variation in pressure of the fluid flow over the top of the surface of Hyperloop vehicle. In Figure 11, the maximum fluid flow pressure is observed on the top of front edge of the Rectangular model of Hyperloop vehicle but throughout the course of flow over the top of capsule the maximum fluid flow pressure is observed in the Elliptical model, followed by Semicircular, Linear and Rectangular models.
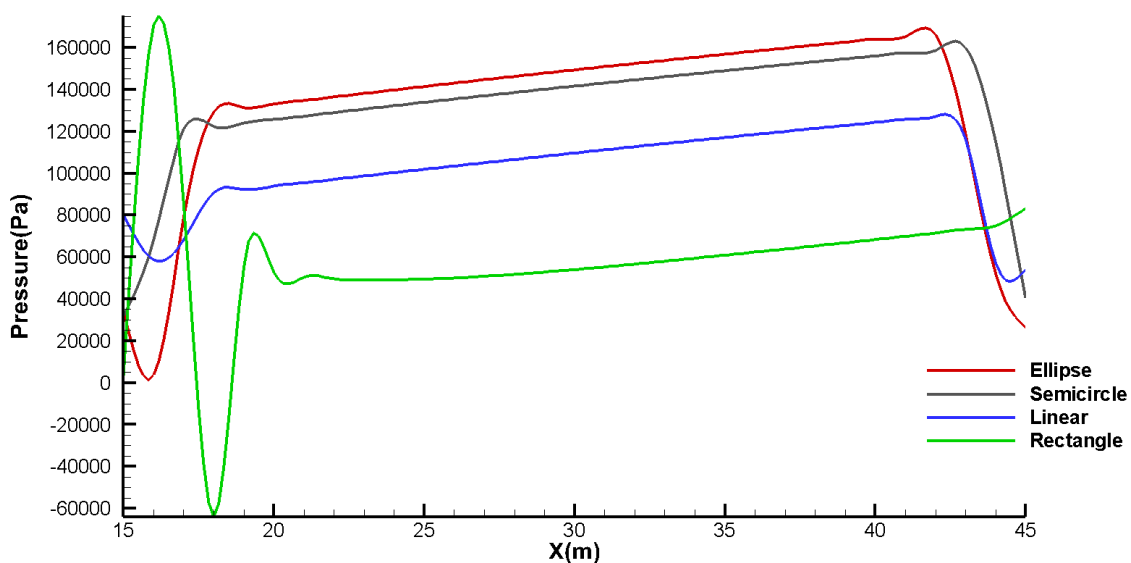
Fig. 11. Pressure profile over the top of the surface of capsule

Figure 12 shows the variation in velocity of the fluid flow over the top of the surface of Hyperloop vehicle. In Figure 12, the peak velocity value of Rectangular model shows the sudden thrust generated due to the high pressure created on the front edge of Rectagular Hyperloop vehicle. The other 3 models show a similar smooth pattern of fluid flow velocity over the top of surface of the Hyperloop vehicle.
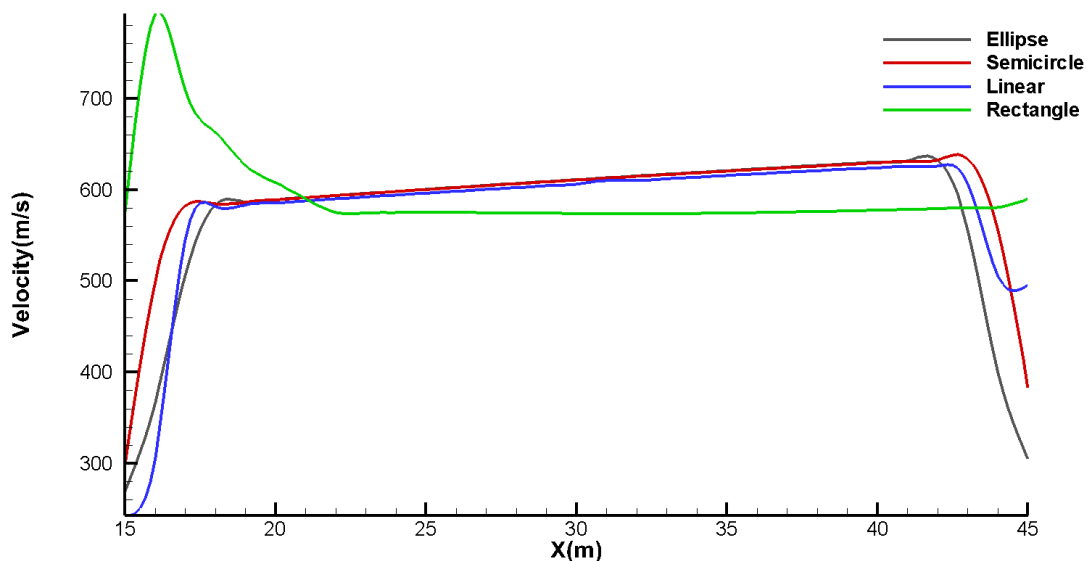
Fig. 12. Velocity profile over the top of the surface of capsule

Figure 13 represents the temporal variation in drag force for different capsule models considered. The drag force is found highest for the Rectangular model of capsule, followed by Linear, Semicircular and Elliptical model.

Fig. 13. Variation in Drag force for different capsule models

The percentage reduction in drag force with reference to Rectangular model of capsule is as following

Table 3
Percentage reduction in Drag force

Capsule Model	Percentage decrease
Linear	58.5
Semi-circular	73.6
Elliptical	75.9

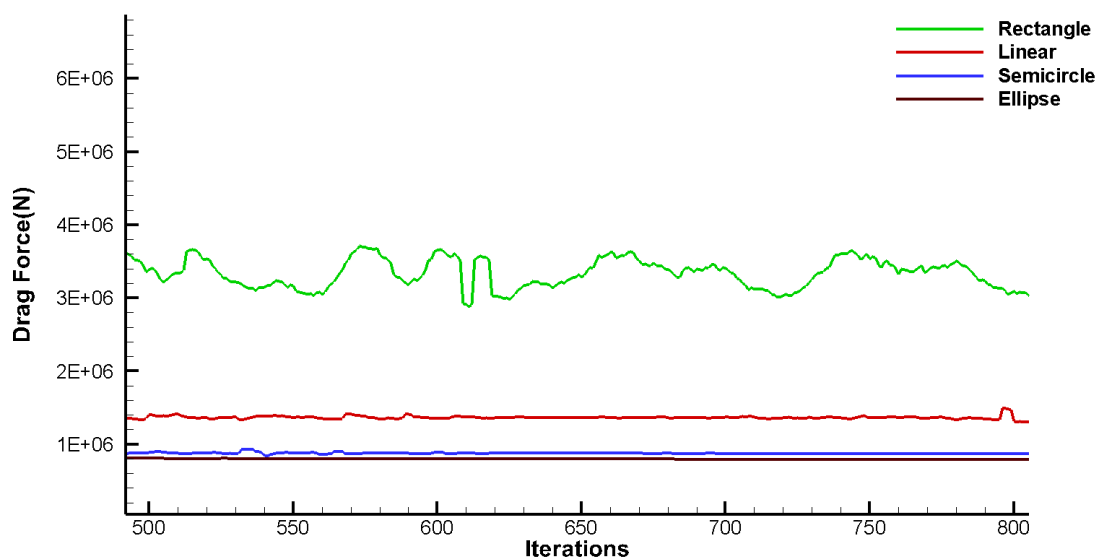According to the findings of all four simulations from Figure 3 to Figure 10, fluid flow pressure is at its lowest at the places on the pod surface where fluid flow velocity is at its highest. This is compatible with the fluid dynamics equation of conservation of energy, which implies that flow velocity and flow pressure are inversely related.

Table 4 shows the comparison of simulation results in terms of Maximum velocity, Maximum pressure and Drag force for all the four investigated models of Hyperloop vehicle.

Table 4
Simulation results for 4 different capsule models

Parameters	Rectangular	Linear	Semi-circular	Elliptical
Maximum Pressure (Pa)	2.23×10^5	1.13×10^5	8.60×10^4	7.78×10^4
Maximum Velocity (m/s)	863	674	634	633
Drag Force (KN)	3388.41	1398.920	885.39	806.45

4. Conclusion

This study compares four possible designs for the Hyperloop capsule model (Rectangular, Linear, Semicircular and Elliptical) and conducts 2-Dimensional CFD simulations of a specific flow field around the Hyperloop capsule. We were able to distinguish the aerodynamic drag, velocity distribution, and pressure distribution by comparing the various types of capsule models, which helped us in selecting the best form of capsule model. ANSYS Fluent was used to analyze the different capsule models using a 2-Dimensional axisymmetric model. The Hyperloop vehicle has a designed speed of 800 Km/h. The tube has a stationary and adiabatic wall surrounding the Hyperloop capsule with 2000 Pa at temperature of 293 K. The 2-Dimensional geometry was analyzed in turbulent k-epsilon Realizable model, with the turbulence intensity = 5% and Turbulence viscosity ratio = 10. Tecplot was used for plotting the results of Drag force, Pressure profiles and Velocity profiles.

i. The Pressure contours show that the maximum fluid flow pressure is observed in the upstream side of Hyperloop vehicle, where the maximum pressure value was observed in Rectangular Capsule model (Max. Pressure = 2.23×10^5 Pa), followed by Linear (1.13×10^5 Pa), Semi-circular (8.60×10^4 Pa) and Elliptical model (7.78×10^4 Pa). These high pressure values observed in the upstream side of vehicle cause obstruction to the fluid flow.

ii. The Velocity contours display the fluid flow velocity throughout the tube. The velocity contour of Rectangular model was observed to have the maximum flow velocity (863m/s) on the edges of the front wall of Hyperloop vehicle, while on observing the other different capsule models they displayed a much consistent fluid flow throughout the flow pattern, with Elliptical model having the least value for maximum velocity (633m/s), followed by Semi-circular (634m/s) and Linear capsule model (674m/s).

iii. The graphs for Pressure and Velocity profiles clearly indicate the disturbance caused to the fluid flow in case of Rectangular capsule model. The Pressure profiles in the graph display that the Elliptical model maintains a higher pressure value over the top of the surface of Hyperloop vehicle in comparison to other capsule models.

iv. The graph displaying the variations in Drag force for the different capsule models shows that the Rectangular capsule model is maintaining a Drag force value of around 3388.41 KN, followed by the Linear (1398.92 KN), Semi-circular (885.39 KN) and Elliptical capsule

model (806.45 KN). In difference to Elliptical and Rectangular model there is a 420% increase in Drag force.

These derived observations clearly suggest that the shape profiles of Hyperloop vehicles have varied effects on their aerodynamic activity and an optimum Hyperloop capsule model can be obtained by improving their aerodynamic behaviors. By comparing the different capsule models, we found out that the Elliptical capsule model can dramatically decrease the aerodynamic drag.

The results of this research study will be very helpful for the development of Hyperloop vehicles in the coming decades. By selecting the suitable capsule design, researchers can now build Hyperloop vehicles with the best aerodynamic characteristics. A systematically designed capsule results in overall considerable energy savings by minimizing the amount of electrical energy required by linear accelerators to propel the Hyperloop, in addition to providing higher aerodynamic qualities to achieve faster speed.

References
[1] Hansen, Ingo A. "Hyperloop transport technology assessment and system analysis." *Transportation Planning and Technology* 43, no. 8 (2020): 803-820. https://doi.org/10.1080/03081060.2020.1828935
[2] Opgenoord, Max M. J., and Philip C. Caplan. "Aerodynamic design of the hyperloop concept." *AIAA Journal* 56, no. 11 (2018): 4261-4270. https://doi.org/10.2514/1.J057103
[3] Zhou, Zhiwei, Chao Xia, Xizhuang Shan, and Zhigang Yang. "Numerical Study on the Aerodynamics of the Evacuated Tube Transportation System from Subsonic to Supersonic." *Energies* 15, no. 9 (2022): 3098. https://doi.org/10.3390/en15093098
[4] Musk, E. "Hyperloop Alpha." *SpaceX*, 2013. http://www.spacex.com/sites/spacex/files/hyperloop_alpha.pdf.
[5] Ross, Philip E. "Hyperloop: no pressure." *IEEE Spectrum* 53, no. 1 (2015): 51-54. https://doi.org/10.1109/MSPEC.2016.7367468
[6] Sui, Yang, Jiqiang Niu, Yanping Yuan, Qiujun Yu, Xiaoling Cao, Dan Wu, and Xiaofeng Yang. "An aerothermal study of influence of blockage ratio on a supersonic tube train system." *Journal of Thermal Science* 31 (2020): 529-540. https://doi.org/10.1007/s11630-020-1281-7
[7] Yang, Yi, Huida Zhang, and Zhaodi Hong. "Research on optimal design method for drag reduction of vacuum pipeline vehicle body." *International Journal of Computational Fluid Dynamics* 33, no. 1-2 (2019): 77-86. https://doi.org/10.1080/10618562.2019.1601711
[8] Srivastava, Prateek, Sachin Kansal, Ashish Talwalkar, and R. Harish. "CFD analysis on the influence of angle of attack on vertical axis wind turbine aerodynamics." In *IOP Conference Series: Earth and Environmental Science*, vol. 850, no. 1, p. 012027. IOP Publishing, 2021. https://doi.org/10.1088/1755-1315/850/1/012027
[9] Harish, R., and K. Venkatasubbaiah. "Numerical investigation of instability patterns and nonlinear buoyant exchange flow between enclosures by variable density approach." *Computers & Fluids* 96 (2014): 276-287. https://doi.org/10.1016/j.compfluid.2014.03.026
[10] Harish, Rajan, and Kondapalli Venkatasubbaiah. "Large Eddy Simulation of thermal plume behavior in horizontally partitioned dual enclosure." In *Building Simulation*, vol. 8, no. 2, pp. 137-148. Tsinghua University Press, 2015. https://doi.org/10.1007/s12273-014-0198-z
[11] Zhang, Yaoping, Daryl Oster, Masayuki Kumada, Jianye Yu, and Shengshan Li. "Key vacuum technology issues to be solved in evacuated tube transportation." *Journal of Modern Transportation* 19, no. 2 (2011): 110-113. https://doi.org/10.1007/BF03325748
[12] Lluesma-Rodríguez, Federico, Temoatzin González, and Sergio Hoyas. "CFD simulation of a hyperloop capsule inside a low-pressure environment using an aerodynamic compressor as propulsion and drag reduction method." *Applied Sciences* 11, no. 9 (2021): 3934. https://doi.org/10.3390/app11093934
[13] Chen, Xuyong, Lifeng Zhao, Jiaqing Ma, and Yuansen Liu. "Aerodynamic simulation of evacuated tube maglev trains with different streamlined designs." *Journal of Modern Transportation* 20, no. 2 (2012): 115-120. https://doi.org/10.1007/BF03325788

[14] Ehrendorfer, K., M. Reiterer, and H. Sockel. "Numerical investigation of the micro pressure wave." In *TRANSAERO-A European Initiative on Transient Aerodynamics for Railway System Optimisation*, pp. 321-341. Springer, Berlin, Heidelberg, 2002. https://doi.org/10.1007/978-3-540-45854-8_26

[15] Kwon, Hyeok-Bin, Ki-Hyeok Jang, Yu-Shin Kim, Kwan-jung Yee, and Dong-Ho Lee. "Nose shape optimization of high-speed train for minimization of tunnel sonic boom." *JSME International Journal Series C Mechanical Systems, Machine Elements and Manufacturing* 44, no. 3 (2001): 890-899. https://doi.org/10.1299/jsmec.44.890

[16] Liu, Jiali, Jiye Zhang, and Weihua Zhang. "Analysis of aerodynamic characteristics of high-speed trains in the evacuated tube." *Journal of Mechanical Engineering* 49, no. 22 (2013): 137-143. https://doi.org/10.3901/JME.2013.22.137

[17] Jia, Wenguang, Kai Wang, Aiping Cheng, Xiangxin Kong, Xing Cao, and Qingling Li. "Air flow and differential pressure characteristics in the vacuum tube transportation system based on pressure recycle ducts." *Vacuum* 150 (2018): 58-68. https://doi.org/10.1016/j.vacuum.2017.12.023

[18] Bao, Shijie, Xiao Hu, Jukun Wang, Tianhao Ma, Yingyu Rao, and Zigang Deng. "Numerical study on the influence of initial ambient temperature on the aerodynamic heating in the tube train system." *Advances in Aerodynamics* 2, no. 1 (2020): 1-18. https://doi.org/10.1186/s42774-020-00053-8

[19] Chu, Chia-Ren, Ssu-Ying Chien, Chung-Yue Wang, and Tso-Ren Wu. "Numerical simulation of two trains intersecting in a tunnel." *Tunnelling and Underground Space Technology* 42 (2014): 161-174. https://doi.org/10.1016/j.tust.2014.02.013

[20] Kim, Joon-Hyung, and Joo-Hyun Rho. "Pressure wave characteristics of a high-speed train in a tunnel according to the operating conditions." *Proceedings of the Institution of Mechanical Engineers, Part F: Journal of Rail and Rapid Transit* 232, no. 3 (2018): 928-935. https://doi.org/10.1177/0954409717702015

[21] Zhou, Peng, Jiye Zhang, Tian Li, and Weihua Zhang. "Numerical study on wave phenomena produced by the super high-speed evacuated tube maglev train." *Journal of Wind Engineering and Industrial Aerodynamics* 190 (2019): 61-70. https://doi.org/10.1016/j.jweia.2019.04.003

[22] Niu, Jiqiang, Yang Sui, Qiujun Yu, Xiaoling Cao, and Yanping Yuan. "Numerical study on the impact of Mach number on the coupling effect of aerodynamic heating and aerodynamic pressure caused by a tube train." *Journal of Wind Engineering and Industrial Aerodynamics* 190 (2019): 100-111. https://doi.org/10.1016/j.jweia.2019.04.001

[23] Kale, Sanket R., Yogesh N. Laghane, Akash K. Kharade, and Supriya B. Kadus. "Hyperloop: advance mode of transportation system and optimize solution on traffic congestion." *International Journal for Research in Applied Science & Engineering Technology (IJRASET)* 7, no. 7 (2019): 539-552. https://doi.org/10.22214/ijraset.2019.7085

[24] Pathan, Khizar Ahmed, Prakash S. Dabeer, and Sher Afghan Khan. "Investigation of base pressure variations in internal and external suddenly expanded flows using CFD analysis." *CFD Letters* 11, no. 4 (2019): 32-40.

[25] Gan, Edwin Chern Junn, Mikhail Fong, and Yee Luon Ng. "CFD Analysis of Slipstreaming and Side Drafting Techniques Concerning Aerodynamic Drag in NASCAR Racing." *CFD Letters* 12, no. 7 (2020): 1-16. https://doi.org/10.37934/cfdl.12.7.116

[26] Khalil, Mohamed F., Sadek Z. Kassab, Ihab G. Adam, and Mohamed A. Samaha. "Prediction of lift and drag coefficients on stationary capsule in pipeline." *CFD Letters* 1, no. 1 (2009): 15-28.

[27] Abobaker, Mostafa, Abdulhafid M. Elfaghi, and Sogair Addeep. "Numerical Study of Wind-Tunnel Wall Effects on Lift and Drag Characteristics of NACA 0012 Airfoil." *CFD Letters* 12, no. 11 (2020): 72-82. https://doi.org/10.37934/cfdl.12.11.7282

[28] Zakher, Bassem Nashaat, Mostafa El-Hadary, and Andrew Nabil Aziz. "The effect of vortex generators on aerodynamics for sedan cars." *CFD Letters* 11, no. 6 (2019): 1-17.

[29] Harish, R. "Buoyancy driven turbulent plume induced by protruding heat source in vented enclosure." *International Journal of Mechanical Sciences* 148 (2018): 209-222. https://doi.org/10.1016/j.ijmecsci.2018.09.001

[30] Harish, R. "Effect of heat source aspect ratio on turbulent thermal stratification in a naturally ventilated enclosure." *Building and Environment* 143 (2018): 473-486. https://doi.org/10.1016/j.buildenv.2018.07.043

[31] Waman, W., and R. Harish. "Influence of volume blockage ratio on turbulent buoyant plume dispersion in mixed ventilated tunnel." *Journal of Wind Engineering and Industrial Aerodynamics* 207 (2020): 104397. https://doi.org/10.1016/j.jweia.2020.104397

[32] Pandey, Brijesh Kumar, and Sujay Kumar Mukherjea. "Aerodynamic simulation of evacuated tube transport trains with suction at tail." In *ASME International Mechanical Engineering Congress and Exposition*, vol. 46613, p. V012T15A036. American Society of Mechanical Engineers, 2014. https://doi.org/10.1115/IMECE2014-37904

[33] Versteeg, Henk Kaarle, and Weeratunge Malalasekera. *An introduction to computational fluid dynamics: the finite volume method*. Pearson Education, 2007.